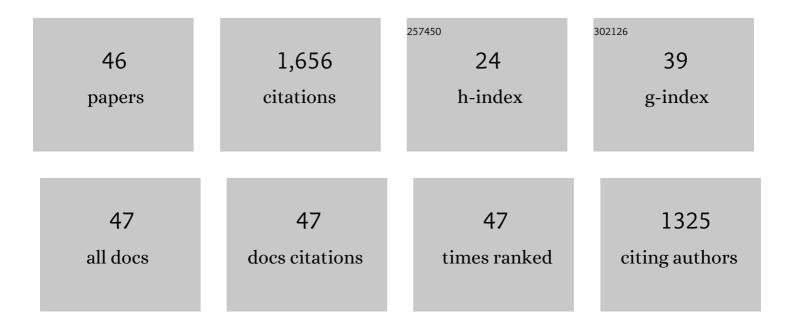
Ivan Koulakov

List of Publications by Year in descending order

Source: https://exaly.com/author-pdf/11197861/publications.pdf Version: 2024-02-01



#	Article	IF	CITATIONS
1	High-frequency <i>P</i> and <i>S</i> velocity anomalies in the upper mantle beneath Asia from inversion of worldwide traveltime data. Journal of Geophysical Research, 2011, 116, .	3.3	115
2	Rapid changes in magma storage beneath the Klyuchevskoy group of volcanoes inferred from time-dependent seismic tomography. Journal of Volcanology and Geothermal Research, 2013, 263, 75-91.	2.1	100
3	Seismic tomographic imaging ofP- andS-waves velocity perturbations in the upper mantle beneath Iran. Geophysical Journal International, 2007, 169, 1089-1102.	2.4	80
4	Moho depth and three-dimensionalPandSstructure of the crust and uppermost mantle in the Eastern Mediterranean and Middle East derived from tomographic inversion of local ISC data. Geophysical Journal International, 2006, 164, 218-235.	2.4	77
5	4D Arctic: A Glimpse into the Structure and Evolution of the Arctic in the Light of New Geophysical Maps, Plate Tectonics and Tomographic Models. Surveys in Geophysics, 2014, 35, 1095-1122.	4.6	70
6	Velocity structure around the Baikal rift zone from teleseismic and local earthquake traveltimes and geodynamic implications. Tectonophysics, 1998, 296, 125-144.	2.2	64
7	<i>P</i> , <i>S</i> velocity and <i>V_P</i> / <i>V_S</i> ratio beneath the Toba caldera complex (Northern Sumatra) from local earthquake tomography. Geophysical Journal International, 2009, 177, 1121-1139.	2.4	63
8	Feeding volcanoes of the Kluchevskoy group from the results of local earthquake tomography. Geophysical Research Letters, 2011, 38, .	4.0	63
9	P- andS-velocity images of the lithosphere-asthenosphere system in the Central Andes from local-source tomographic inversion. Geophysical Journal International, 2006, 167, 106-126.	2.4	62
10	Anisotropic structure beneath central Java from local earthquake tomography. Geochemistry, Geophysics, Geosystems, 2009, 10, .	2.5	61
11	Delamination or slab detachment beneath Vrancea? New arguments from local earthquake tomography. Geochemistry, Geophysics, Geosystems, 2010, 11, .	2.5	55
12	Three different types of plumbing system beneath the neighboring active volcanoes of Tolbachik, Bezymianny, and Klyuchevskoy in Kamchatka. Journal of Geophysical Research: Solid Earth, 2017, 122, 3852-3874.	3.4	53
13	Mechanism of the Andean Orogeny: Insight from Numerical Modeling. , 2006, , 513-535.		50
14	Breathing of the Nevado del Ruiz volcano reservoir, Colombia, inferred from repeated seismic tomography. Scientific Reports, 2017, 7, 46094.	3.3	49
15	Structure and dynamics of the upper mantle beneath the Alpine–Himalayan orogenic belt, from teleseismic tomography. Tectonophysics, 2002, 358, 77-96.	2.2	48
16	The feeder system of the Toba supervolcano from the slab to the shallow reservoir. Nature Communications, 2016, 7, 12228.	12.8	47
17	Fluid ascent during the 2004–2005 unrest at Mt. Spurr inferred from seismic tomography. Geophysical Research Letters, 2013, 40, 4579-4582.	4.0	45
18	Upper mantle structure beneath the Siberian craton and surrounding areas based on regional tomographic inversion of P and PP travel times. Tectonophysics, 2010, 486, 81-100.	2.2	44

Ivan Koulakov

#	Article	IF	CITATIONS
19	Evidence for high fluid/melt content beneath Krakatau volcano (Indonesia) from local earthquake tomography. Journal of Volcanology and Geothermal Research, 2011, 206, 96-105.	2.1	38
20	Seismic structure changes beneath Redoubt Volcano during the 2009 eruption inferred from local earthquake tomography. Journal of Geophysical Research: Solid Earth, 2014, 119, 4938-4954.	3.4	36
21	Fluid ascent and magma storage beneath Gunung Merapi revealed by multi-scale seismic imaging. Journal of Volcanology and Geothermal Research, 2013, 261, 7-19.	2.1	34
22	Structural cause of a missed eruption in the Harrat Lunayyir basaltic field (Saudi Arabia) in 2009. Geology, 2015, 43, 395-398.	4.4	30
23	Evidence for anomalous mantle upwelling beneath the Arabian Platform from travel time tomography inversion. Tectonophysics, 2016, 667, 176-188.	2.2	29
24	Mantle and Crustal Sources of Magmatic Activity of Klyuchevskoy and Surrounding Volcanoes in Kamchatka Inferred From Earthquake Tomography. Journal of Geophysical Research: Solid Earth, 2020, 125, e2020JB020097.	3.4	29
25	Anisotropic tomography of Hokkaido reveals delaminationâ€induced flow above a subducting slab. Journal of Geophysical Research: Solid Earth, 2015, 120, 3219-3239.	3.4	27
26	Structure of Volatile Conduits beneath Gorely Volcano (Kamchatka) Revealed by Local Earthquake Tomography. Geosciences (Switzerland), 2017, 7, 111.	2.2	25
27	Magmatic and Sedimentary Structure beneath the Klyuchevskoy Volcanic Group, Kamchatka, From Ambient Noise Tomography. Journal of Geophysical Research: Solid Earth, 2020, 125, e2019JB018900.	3.4	23
28	Three-dimensional seismic structure of the upper mantle beneath the central part of the Eurasian continent. Geophysical Journal International, 1998, 133, 467-489.	2.4	22
29	Studying deep sources of volcanism using multiscale seismic tomography. Journal of Volcanology and Geothermal Research, 2013, 257, 205-226.	2.1	21
30	Unrest of the Udina volcano in Kamchatka inferred from the analysis of seismicity and seismic tomography. Journal of Volcanology and Geothermal Research, 2019, 379, 45-59.	2.1	21
31	Teleseismic tomography reveals no signature of the Dead Sea Transform in the upper mantle structure. Earth and Planetary Science Letters, 2006, 252, 189-200.	4.4	20
32	Anatomy of the Bezymianny volcano merely before an explosive eruption on 20.12.2017. Scientific Reports, 2021, 11, 1758.	3.3	19
33	Creating realistic models based on combined forward modeling and tomographic inversion of seismic profiling data. Geophysics, 2010, 75, B115-B136.	2.6	18
34	Focused magmatism beneath Uturuncu volcano, Bolivia: Insights from seismic tomography and deformation modeling. , 2017, 13, 1855-1866.		17
35	Seismic structure beneath the Gulf of Aqaba and adjacent areas based on the tomographic inversion of regional earthquake data. Solid Earth, 2016, 7, 965-978.	2.8	16
36	Evolution of the Magma Conduit Beneath the Galeras Volcano Inferred From Repeated Seismic Tomography. Geophysical Research Letters, 2018, 45, 7514-7522.	4.0	16

Ιναν Κουιακον

#	Article	IF	CITATIONS
37	Threeâ€dimensional seismic anisotropy in the crust and uppermost mantle beneath the Taiwan area revealed by passive source tomography. Journal of Geophysical Research: Solid Earth, 2015, 120, 7814-7829.	3.4	14
38	Application of repeated passive source travel time tomography to reveal weak velocity changes related to the 2011 Tohokuâ€Oki <i>M_w</i> 9.0 earthquake. Journal of Geophysical Research: Solid Earth, 2016, 121, 4408-4426.	3.4	9
39	Ongoing formation of felsic lower crustal channel by relamination in Zagros collision zone revealed from regional tomography. Scientific Reports, 2020, 10, 8224.	3.3	9
40	Seismic Tomography of Volcanoes. , 2021, , 1-18.		8
41	Seismic Tomography of Volcanoes. , 2015, , 3117-3134.		6
42	Pathways of volatile migration in the crust beneath Harrat Lunayyir (Saudi Arabia) during the unrest in 2009 revealed by attenuation tomography. Journal of Volcanology and Geothermal Research, 2017, 330, 1-13.	2.1	5
43	Numerical modelling of seismic waves from earthquakes recorded by a network on ice floes. Geophysical Journal International, 2019, 218, 74-87.	2.4	5
44	Multiscale Seismic Tomography Imaging of Volcanic Complexes. , 2012, , .		4
45	Sources of the eruption of Kambalny volcano (Southern Kamchatka) in March 2017 inferred from local earthquake tomography. Journal of Volcanology and Geothermal Research, 2021, 420, 107392.	2.1	4
46	Finding a realistic velocity distribution based on iterating forward modelling and tomographic inversion. Geophysical Journal International, 2011, 186, 349-358.	2.4	3